It is advisable to refer to the publisher's version if you intend to cite from the work.
https://doi.org/10.1088/1742-6596/1107/4/042023

For information about Research at UCLan please go to http://www.uclan.ac.uk/research/

PAPER • OPEN ACCESS

Experimental investigation of externally venting flames geometric characteristics and impact on the façade of corridor-like enclosures

IOP ebooks™

Bringing you innovative digital publishing with leading voices to create your essential collection of books in STEM research.

Start exploring the collection - download the first chapter of every title for free.

Experimental investigation of externally venting flames geometric characteristics and impact on the façade of corridor-like enclosures

Konstantinos CHOTZOGLOU[1], Eleni ASIMAKOPOULOU[1], Jianping ZHANG[1], Michael DELICHATSIOS[1,2]

[1] *FireSERT, Belfast School of Architecture and the Built Environment, Ulster University, United Kingdom*

[2] *Currently: Northeastern University, Boston, USA and*

University of Science and Technology of China (USTC), Hefei, China

e.asimakopoulou@ulster.ac.uk

ABSTRACT

Understanding of the physics and mechanisms of fire development and externally venting flames (EVF) in corridor-like enclosures is fundamental to studying fire spread to adjacent floors in high-rise buildings. This work aims to investigate the burning behaviour of a liquid fuel pool fire in a corridor-like enclosure and to identify the key factors influencing EVF characteristics and its impact on façades. A series of experiments is conducted in a medium-scale corridor-facade configuration using ethanol pool fires. A new fuel supply system has been developed to keep the fuel level constant to minimize lip effects. The influence of fuel surface area and ventilation factor on the fire development is also investigated. Experimental measurements consist of mass loss, heat release rate, temperatures and heat fluxes inside the corridor and on the facade. Three distinct burning regions are observed and their characteristics depend on both the pan size and ventilation factor. A power dependence of EVF height in relation to excess external heat release rate has been found. The impact of EVF on the façade is investigated by measuring heat flux on the façade using thin steel plate probes. It is found that the characteristics of EVF strongly depend on opening dimensions and for large opening widths EVF tend to emerge from the opening as two separate fire plumes.

KEYWORDS:

liquid pool fire, corridor-like enclosure, façade fire, flame height, heat flux

INTRODUCTION

Understanding of the physics and mechanisms of fire development in enclosures and flames emerging through openings is fundamental to studying fire spread to adjacent floors or buildings. Recent high-rise building fires around the world highlight the importance of understanding the mechanisms of fire spread not only at the interior of buildings but also those due to Externally Venting Flames (EVF) [1,2]. Consequences of EVF induced fire events include loss of life and injuries, health impact through smoke exposure, property and infrastructure loss, business interruption, ecosystem degradation, soil erosion and huge firefighting costs [1]. Though substantial research has been conducted on fire characteristics in typical cubic-like compartments [3], there is still limited data on the development of enclosure fires and EVF in other geometries (e.g. long corridors, tunnels etc). For the few studies in corridor-like enclosures [4,5], gaseous fuels were used. As the mass flow rate (thus heat release rate) of gaseous fuels must be pre-defined, it does not consider the interaction between the flame, the hot gas layer and the pyrolysis rate of the fuel, which is of fundamental importance in growth and development of real fires. This work investigates the burning behaviour of a liquid fuel pool fire in a corridor-like enclosure and the heat impact of the subsequent externally venting flames (EVF) on the façade. The effects of the size and location of the pool fire and the dimensions of the opening on the burning characteristics of the EVF are examined. Experimental measurements consist of mass loss, heat release rate, temperatures and heat fluxes inside the corridor and on the façade. Correlations are developed for external flame height of EVF and heat flux on the façade and compared to the ones obtained using gaseous fuels [4,5].

EXPERIMENTAL DETAILS

Corridor-like enclosure and façade configuration

Experiments were conducted in a medium-scale corridor-facade configuration having internal dimensions 3 m x 0.5 m x 0.5 m and a 1.8 m x 1 m façade was attached to the front box. High tempered 40 mm resistant boards were used as inner corridor lining and exposed side of façade; the outer walls were constructed using 12 mm MDF boards. A schematic of the experimental facility, illustrating the locations of the employed measuring devices, is given in Fig. 1. A novel fuel supply system was designed to maintain constant fuel level to minimize lip effects; ethanol was used in a circular sandbox burner positioned at geometrical center of Box A or F. The fuel surface area and ventilation factor (by altering the dimensions of the door-like opening) were varied to examine their effects on the fire development. In total, more than 60 experiments were conducted to ensure repeatability. A summary of the main operational parameters, e.g. burner position, opening size (opening width W_o and opening height H_o), ventilation factor ($A_oH_o^{1/2}$, A_o corresponds to opening area), ventilation regime (Under or Over ventilated, indicated as U or O respectively), length scale ($l_1=(A_oH_o^{1/2})^{2/5}$) [4], total heat release rate (HRR) ($\dot{Q}_{exp}$) and excess HRR ($\dot{Q}_{ex}$) [4] for the experiments presented in this work is shown in Table 1.
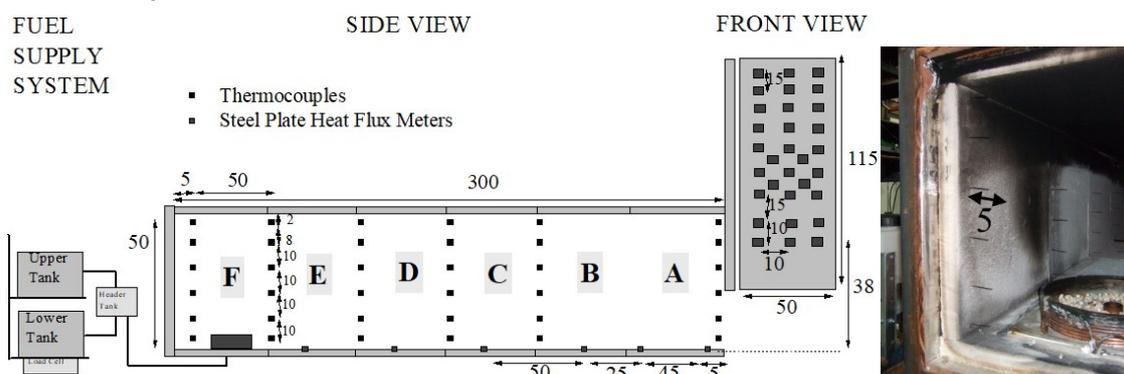

Fig. 1. Fire test configuration and experimental setup (left) and inner corridor lining (right).

Sensors and data acquisition system

Thirty-six K-type 1.5 mm diameter thermocouples are used to monitor gas temperatures inside the enclosure at every 6 s [4,5]. Six thermocouples were positioned 5 cm from the side wall, in each Box, to monitor gas temperature. Steel plates were used to monitor the heat flux on the façade, Fig.1. The experimental set-up was placed under a 3 x 3 m^2 hood to measure $\dot{Q}_{exp}$, production of CO, CO_2 and smoke. Videos were recorded by a CCD camera facing the façade, based on which an in-house developed image processing tool is used to evaluate the geometric characteristics of the façade fires by calculating the average flame probability (intermittency) [6]. The threshold limits for Red, Green and Blue color levels and luminosity were acquired through an extended statistical analysis of the flame ejected from the opening.

Table 1. Summary of main operational parameters for the examined test cases.

a/a	Test	Burner position	Pan diam.	Opening size	$A_oH_o^{1/2}$	Vent. Regime	l_1	$\dot{Q}_{exp}$	$\dot{Q}_{ex}$	z_f
		Box	m	m x m	$cm^{5/2}$		-	kW	kW	m
1	FR20W20xH20	A	0.2	0.20x0.20	0.0179	O	0.20	12.1	-	0.11
2	FR20W25xH25	A	0.2	0.25x0.25	0.0313	O	0.25	21.5	-	0.21
3	FR30W10xH25	A	0.3	0.10x0.25	0.0125	U	0.17	22.2	-	0.22
4	FR30W20xH20	A	0.3	0.20x0.20	0.0179	O	0.20	17.0	-	0.13
5	FR30W25xH25	A	0.3	0.25x0.25	0.0313	O	0.25	31.0	-	0.34
6	FR30W30xH30	A	0.3	0.30x0.30	0.0493	U	0.30	56.1	-	0.49
7	FR30W50xH25	A	0.3	0.50x0.25	0.0625	U	0.33	75.1	-	0.48
8	FR30W50xH50	A	0.3	0.50x0.50	0.1768	O	0.50	69.5	-	0.33
9	BC20W25xH25	F	0.2	0.25x0.25	0.0313	U	0.25	39.0	2.5	0.22
10	BC20W30xH30	F	0.2	0.30x0.30	0.0493	U	0.30	68.5	11.1	0.51
11	BC20W50xH25	F	0.2	0.50x0.25	0.0625	U	0.33	74.0	9.0	0.37
12	BC30W25xH25	F	0.3	0.25x0.25	0.0313	U	0.25	39.5	2.9	0.19
13	BC30W30xH30	F	0.3	0.30x0.30	0.0493	U	0.30	70.0	14.0	0.58
14	BC30W50xH25	F	0.3	0.50x0.25	0.0625	U	0.33	77.0	9.0	0.64
15	BC30W50xH50	F	0.3	0.50x0.50	0.1768	O	0.50	105.0	-	0.30

RESULTS AND DISCUSSION

Heat release rate inside the enclosure

A parametric analysis is performed to identify the main parameters influencing the burning behaviour and subsequent EVF, namely pan size, pan location and ventilation factor. To demonstrate the main characteristic stages regarding the fire growth, the temporal evolution of measured *HRR*, $\dot{Q}_{exp}$, and theoretical HRR, $\dot{Q}_{th}$, are plotted in Fig. 2 for two characteristic underventilated test cases, BC20W30xH30 and BC30W30xH30. The theoretical HRR, $\dot{Q}_{th}$, is calculated by multiplying the measured fuel mass loss rate by the heat of combustion of ethanol, 26.78 MJ/kg. The maximum *HRR* in stoichiometric conditions inside an enclosure, $\dot{Q}_{st,in}$, is calculated by multiplying the maximum air inflow rate by the heat released by complete combustion of 1 kg oxygen, which for most fuels is found to be approximately equal to 3000 kJ/kg [7]. To demonstrate the enclosure effect, free-burn ethanol pool fire experiments for the 30 cm (FB30) and 20 cm (FB20) pan are also depicted. Each experiment was terminated by stopping the fuel supply to the pan and closing the openings.
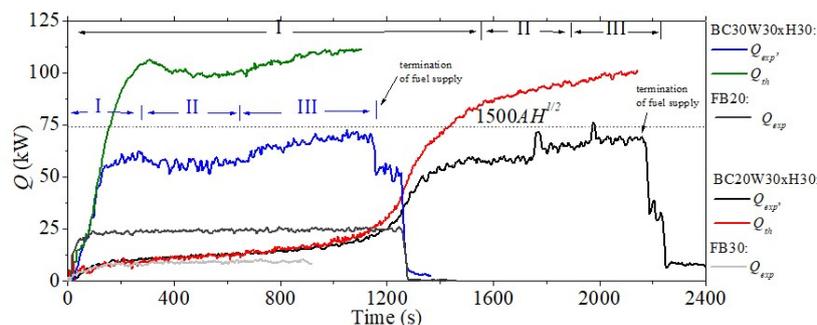

Fig. 2. Temporal evolution of $\dot{Q}_{exp}$ and $\dot{Q}_{th}$ for test cases BC30W30xH30 and BC20W30xH30.

For all under-ventilated fires with the pan located at Box F, as indicatively presented in Fig. 2, the fire behaviour is characterized by three distinct phases namely *Regions I*, *II* and *III* appearing in succession. *Region I* correspond to the fuel-controlled period (growth period), where the combustion efficiency is close to unity and thus $\dot{Q}_{exp}$, and $\dot{Q}_{th}$, are almost equal. After this phase, during *Region II*, fire gradually becomes ventilation-controlled, $\dot{Q}_{exp}$ reaches a plateau until flames ejects through the opening. Note that $\dot{Q}_{exp}$ does not reach the maximum heat released inside the enclosure approaching $1500A_oH_o^{1/2}$ value that has been found for rectangular compartments [3]. This value is decreased, calculated at approximately $1100A_oH_o^{1/2}$, indicating that the amount of air inflow in long corridors is less than in rectangular enclosures with the same opening geometry [8]. Flames ejection, as observed visually and through the image processing algorithm, associated with a sudden increase in the $\dot{Q}_{exp}$, indicates the beginning of *Region III*, where sustained external burning is observed until a plateau is

formed near the end of the test indicating steady state conditions are established. As depicted in *Fig. 2*, not all the excess fuel burns at the exterior of the corridor as the combustion is incomplete and combustion efficiency in *Region III* is calculated at approximately 0.74 for both cases. Pan size has a significant effect on the time to reaching steady burning. In test cases using the smaller pan it takes longer for the walls and gases in the enclosure to be heated. For under-ventilated cases with the fuel pan located near the opening, at Box A, EVF appeared shortly after ignition and as a result the duration of *Regions I* and *II* is considerably reduced. For the under-ventilated cases, the external HRR, $\dot{Q}_{ex}$, is calculated as the difference between the average values of $\dot{Q}_{exp}$ during steady burning in *Region II* and *III* with the assumption that the burning inside the enclosure has reached the steady state before flame ejection.

Gas temperature inside the enclosure

Present analysis focuses on under-ventilated cases with EVF occurrence. Figure 3 shows the spatial mapping of the thermocouple gaseous temperatures inside the corridor at three characteristic time frames representing the three Regions discussed in previous sections for test cases BC30W30xH30 and FR30W30xH30. During *Region I*, low gas temperatures are observed in the lower layer as fresh air enters the enclosure through the opening, located at the right side of the corridor. In BC30W30xH30, during *Region II*, highest temperatures are observed at the vicinity of Boxes E and D indicating that combustion mainly takes place at these locations and flames gradually propagate towards the opening seeking for available oxygen [4, 5]. During *Region III*, the difference of gas temperatures between the upper and lower layers decreases towards the closed end of the corridor, but still, they cannot be assumed uniform inside the corridor. In *Region III*, flames fill the upper layer of the corridor extending towards the opening and eventually emerges from the opening when the *HRR* becomes sufficiently large. In test case FR30W30xH30, temperature stratification in the interior of the corridor is less evident as EVF emerge more quickly from the opening resulting in lower temperatures in Boxes C to F.
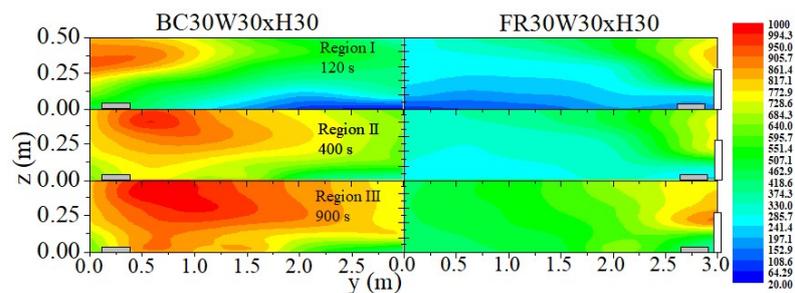

Fig. 3. Spatial visualization of gaseous temperature at the interior of the corridor for test cases F30W30xH30 (left) and B30W30xH30 (right) for 120, 400 and 900s.

EVF height

Figure 4 plots the dimensional flame height, Z_f/l_1, against the dimensionless external heat release rate $\dot{Q}_{ex}^*$ using experimental data from gas burner experiments in rectangular geometries [5], corridors [4] and liquid pool fires in corridors (current study). It is demonstrated that for small flame heights and larger openings the power dependence on the $\dot{Q}_{ex}^*$ calculated following [4] is 2/3, which is in accordance with the physical mechanism corresponding to "wall fire" in which flame is attached to the façade wall or a "half axisymmetric fire" in which flame is detached from the façade wall [5, 9, 10]. For $\dot{Q}_{ex}^* > 1$, experimental results using gas burner from both rectangular and corridor geometries corroborate a 2/5 dependence on $\dot{Q}_{ex}^*$ [5,9,11].
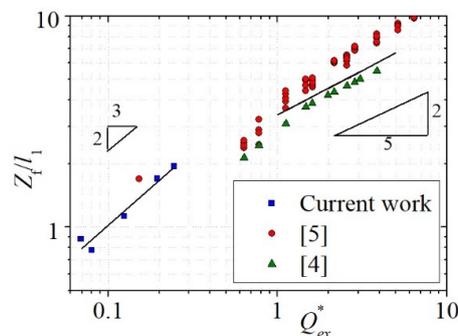

Fig. 4. Flame height correlation for gas burner experiments in rectangular geometries [5] corridors [4] and liquid pool fires in corridors (current study).

Heat fluxes

Figure 5 depicts the vertical distribution of the radiative heat fluxes measured using thin steel plate probes [5,12] at the centreline of the façade for all test cases. Measured heat fluxes decrease with increasing height as expected. The highest heat flux is found always along the centreline except for test cases when the front of the enclosure is completely open, i.e., BC30W50xH50 and FR30W50xH50. As it can be seen from their intermittency contours in Fig. 6, the resulted EVF for these two cases tend to emerge as two separate fire plumes and as a result the maximum heat flux values are off the centreline in contrast to other cases. This finding highlights the influence of the width of the opening, in addition to the ventilation factor, to the resulting EVF shape. For the same opening and pan size, higher heat flux values are observed when the fuel pan is positioned near opening at Box A.
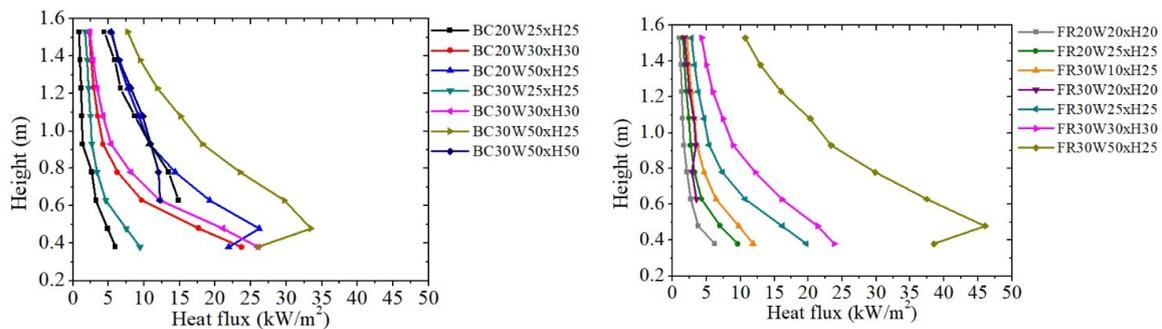

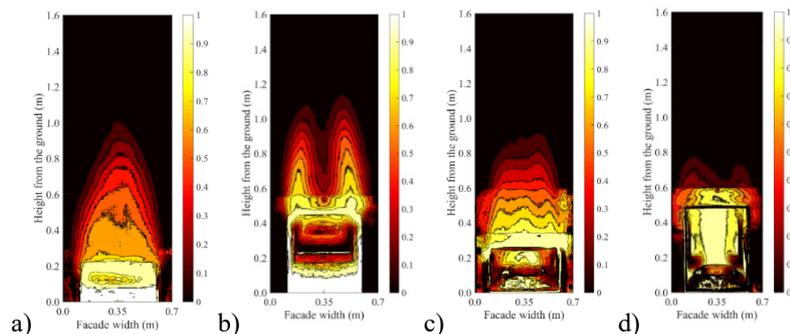Fig. 5. Vertical distribution of heat flux at the centerline of the façade for the BC (left) and FR (right) cases.

Fig. 6. Intermittency contours for a)BC30W50xH25, b)BC3W50x0H50, c)FR30W50xH25, d)FR30W50xH50.

Figure 7 shows the heat flux distributions for under-ventilated cases at the centerline above the opening on façade wall against the value of Z/Z_f, where Z is the location of each steel plate at the centreline as depicted in Fig. 1. Both are measured from the position of neutral plane corresponding to $0.5H_o$ above the bottom of the opening [7]. The residual effect of the aspect ratio of the opening is accounted for by using the exponential factor $\exp(0.60H_o/l_1)$ [4, 5]. It is shown that the measurements of heat flux in this work are mainly located in the intermittent flame and buoyant plume regimes where $Z/Z_f > 0.7$. Despite the scattering of the current data, partially attributed to the different properties of the fuels used, qualitative analysis reveals that current results follow the same trend as Lee's [5] and Beji's [4] data.
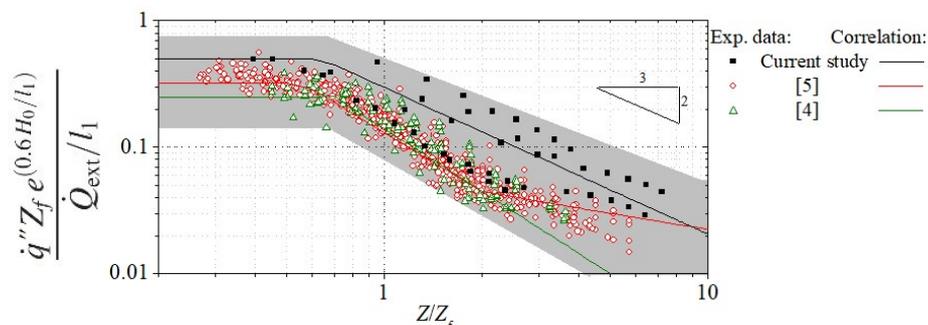

Fig. 7. Dimensionless heat flux against dimensionless height in rectangular geometries [5], corridors [4] and liquid pool fires in corridors (current study).

CONCLUSIONS

We presented an experimental work of liquid pool fires in a reduced-scale corridor-like enclosure, aiming with emphasis to examine the influence of the pool size, location and ventilation openings on the geometric characteristics of EVF and their impact on the façade. The main conclusions are:

1.   Three distinct burning regions (*Region I*, *II* and *III*) were observed based on $\dot{Q}_{exp}$ corresponding respectively to fuel-controlled, ventilation-controlled and steady-state burning.

2.   The location and size of the fuel pan has a strong impact on *HRR* and subsequent EVF characteristics.

3.   For the present cases the dimensionless external heat release rate $\dot{Q}_{ex}^*$ is always less than one, for which a power dependence of the flame height of the EVF on $\dot{Q}_{ex}^*$ is found to be 2/3, compared to 2/5 for larger $\dot{Q}_{ex}^*$ values found for gaseous fuels in previous studies [4,5].

4.   The centreline heat fluxes on the façade are nearly constant just above the opening where the consistent flame region is and subsequently decreases with height. The measurements in this work are mainly located in the intermittent flame and buoyant plume regimes when compared to previous studies using gaseous burner [4,5]. The dimensionless heat fluxes found in this work are generally higher than those reported in [4,5], owing mainly to the uncertainties in the determination of the excess heat release rate.

5.   EVF of the two fully open cases exhibit distinctive characteristics and tend to emerge from the opening as two separate fire plumes resulting in lower heat flux values at the façade centreline.

6.   The overall design of the medium-scale compartment-façade fire tests can be scaled-up provided certain non-dimensional parameters are preserved. Subsequently, correlations derived in the frame of the current research work can be used to enhance façade fire safety design methodologies and after detailed validation can be gradually incorporated in facades prescriptive fire safety regulations.

REFERENCES

[1] White, N., Delichatsios, M. (2014) Fire hazards of exterior wall assemblies containing combustible components, 1st ed., SpringerBriefs in Fire, Springer, New York, U.S.A.

[2] Asimakopoulou, E., Chotzoglou, K., Kolaitis, D., Founti, M. (2016) Characteristics of externally venting flames and their effects on the façade: a detailed experimental study, *Fire Technology* 52:2043-2069, https://doi.org/10.1007/s10694-016-0575-5

[3] Delichatsios, M.A., Silcock, G.W.H., Liu, X., Delichatsios, M., Lee, Y.P. (2004) Mass pyrolysis rates and excess pyrolysate in Fully Developed Enclosure Fires, *Fire Safety Journal* 39:1– 21, https://doi.org/10.1016/j.firesaf.2003.07.006

[4] Beji, T., Ukleja, S., Zhang, J., Delichatsios, M.A. (2012) Fire behaviour and external flames in corridor and tunnel-like enclosures, *Fire and Materials* 36:636-647, https://doi.org/10.1002/fam.1124

[5] Lee, Y.P., Delichatsios, M.A., Silcock, G. (2007) Heat fluxes and flame heights in facades from fires in enclosures of varying geometry, *Proceedings of the Combustion Institute* 31:2521-2528, https://doi.org/10.1016/j.proci.2006.08.033

[6] Asimakopoulou, E., Kolaitis, D., Founti, M. (2016) Geometrical characteristics of externally venting flames: Assessment of fire engineering design correlations using medium-scale compartment-façade fire tests, Journal of Loss Prevention in the Process Industries 44: 780-790, http://dx.doi.org/10.1016/j.jlp.2016.09.006

[7] O'Connor, D., "The Building Envelope: Fire Spread, Construction Features and Loss Examples", SFPE Handbook of Fire Protection Engineering (5th ed.) Hurley M.J., National Fire Protection Association, Quincy, MA 02269, 2016, p 3242/3512.

[8] Yii, E., Fleischmann C., Buchanan, A. (2007) Vent flows in fire compartments with large openings, *Journal of Fire Protection Engineering* 17: 221-237, http://dx.doi.org/10.1177/1042391507069634

[9] Yokoi, S. (1960) Study on the prevention of fire spread caused by hot upward current, Japanese Ministry of Construction, Building Research Institute Report 34, 1960.

[10] Quintiere, J.G., Harkleroad, M., Hasemi, Y. (1986) Wall Flames and Implications for Upward Flame Spread, *Combustion Science and Technology* 48:191–222.

[11] Lu, K. H., Hu, L. H., Tang F., He L. H., Zhang, X. C., Qiu, Z. W. (2014) Heat flux profile upon building facade with side walls due to window ejected fire plume: An experimental investigation and global correlation, Fire Safety Journal 70:14-22, http://dx.doi.org/10.1016/j.firesaf.2014.08.001

[12] Zhang, J., Delichatsios, M. A. (2009) Determination of the convective heat transfer coefficient in three-dimensional inverse heat conduction problems, *Fire Safety Journal* 44: 681-690.